Supporting Information

Synergistic effect of alkali metal doping and thiocyanate passivation in $CsPbBr_3$ for HTM-free all-inorganic perovskite solar cells

Shiqiang Jiang [a,#], Haojie Sui [a,#], Benlin He [a,*], Xinyi Zhang [a], Zhihao Zong [a], Haiyan Chen [a,*], Qunwei Tang [b,*]

[a] School of Materials Science and Engineering, Ocean University of China, Qingdao 266100, PR China. E-mail: blhe@ouc.edu.cn, chenhaiyan@ouc.edu.cn

[b] Institute of Carbon Neutrality, College of Chemical and Biological Engineering, Shandong University of Science and Technology, Qingdao 266590, PR China. E-mail: tangqunwei@jnu.edu.cn

[#] Shiqiang Jiang and Haojie Sui contributed equally to this work.

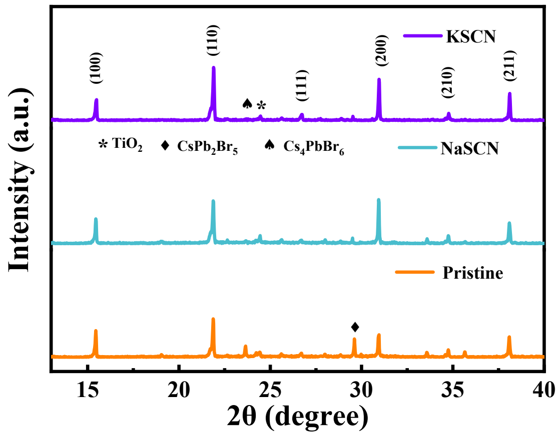

Fig. S1 XRD patterns of various $CsPbBr_3$ films.

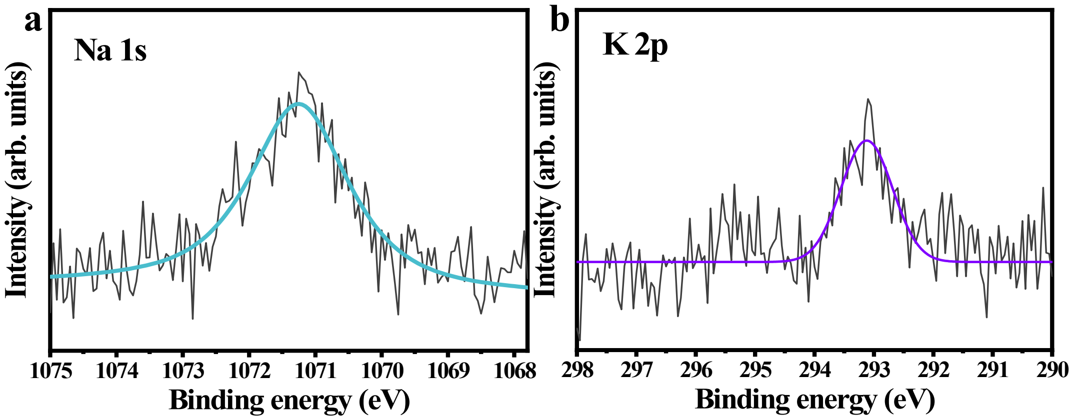

Fig. S2 High-resolution XPS spectra of (a) Na 1s and (b) K 2p of the doped $CsPbBr_3$ films.

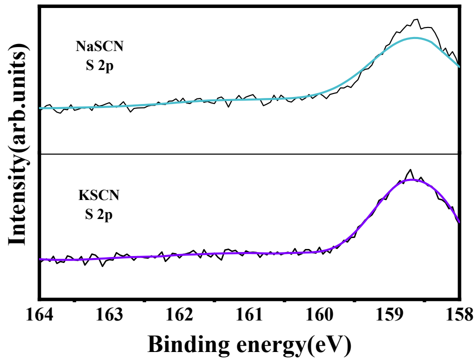

Fig. S3 High-resolution XPS spectra of S 2p of NaSCN and KSCN doped $CsPbBr_3$ films.

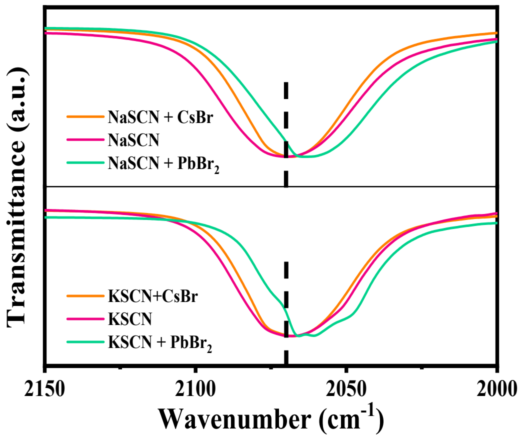

Fig. S4 FTIR spectra of Na/KSCN, Na/KSCN + CsBr and Na/KSCN + $PbBr_2$.

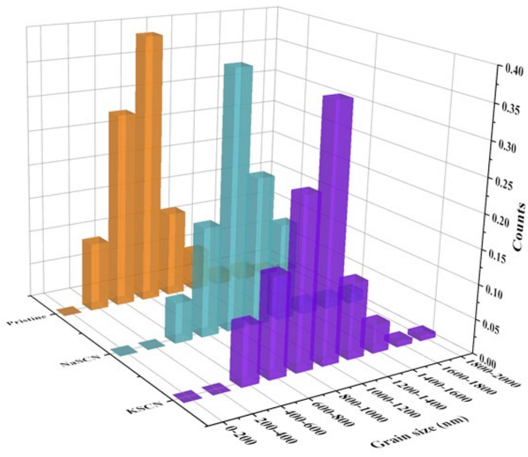

Fig. S5 The grain size distribution of various $CsPbBr_3$ films.

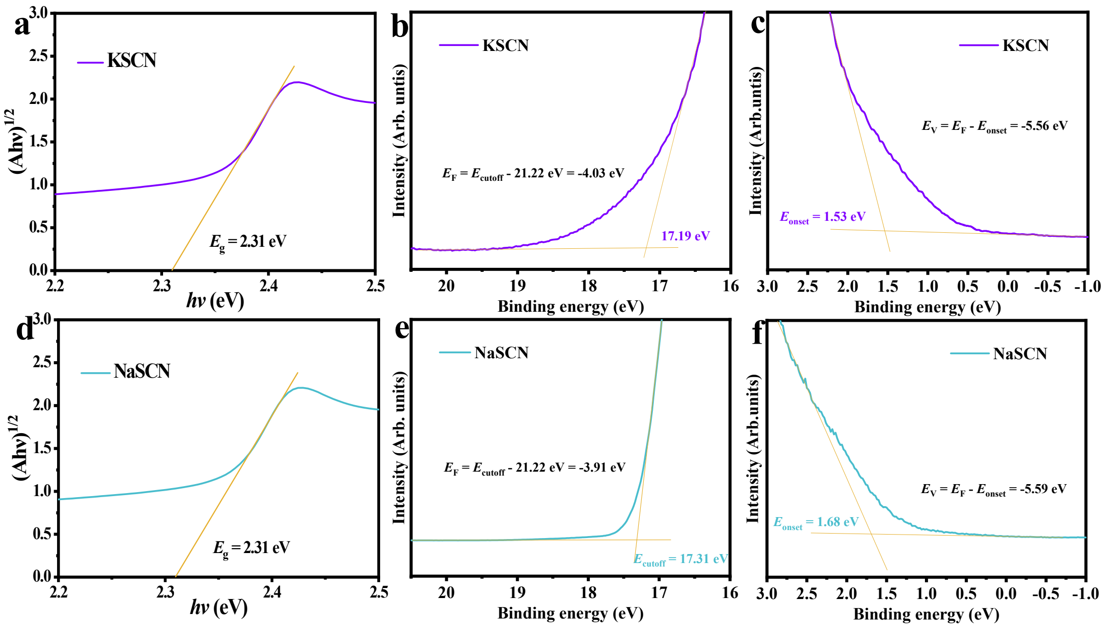

Fig. S6 (a)&(d) Tauc plots, (b)&(e) the secondary electron cutoff and (c)&(f) onset binding energies of NaSCN and KSCN doped $CsPbBr_3$ films.

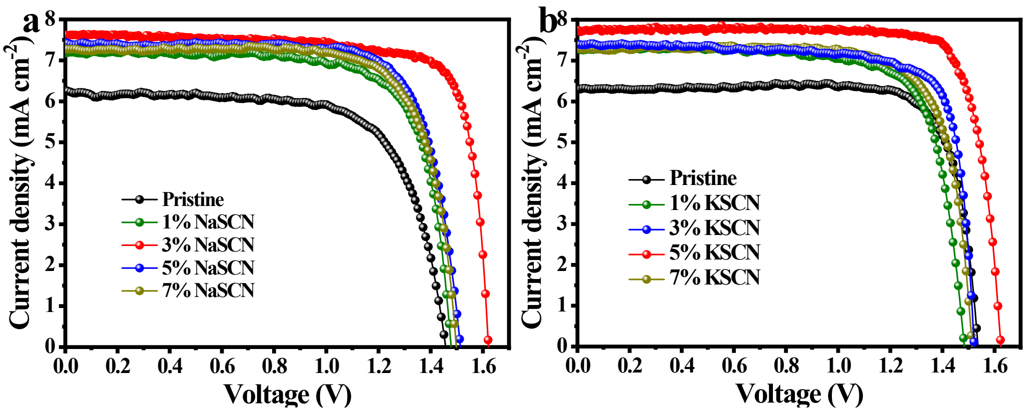

Fig. S7 *J*-*V* curves of HTM-free $CsPbBr_3$ PSCs doped with (a) NaSCN and (b) KSCN at different molar ratio.

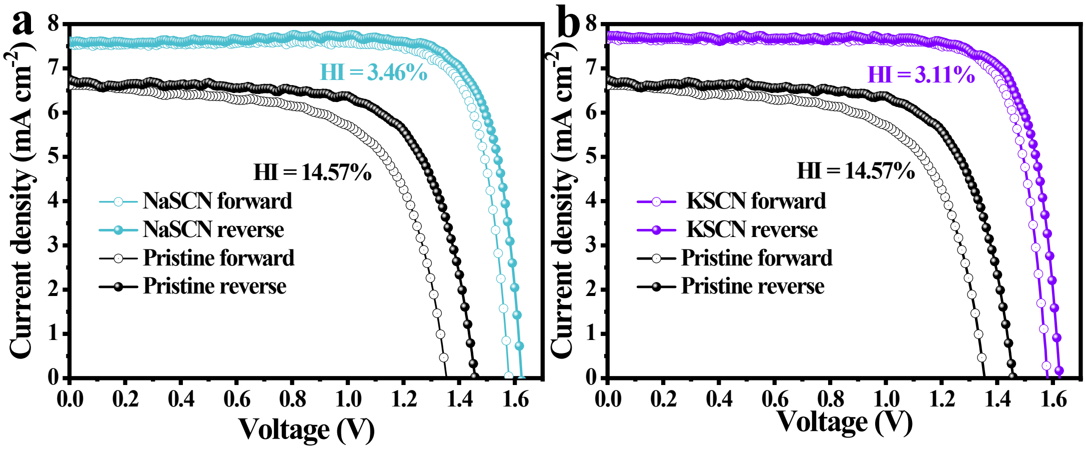

Fig. S8 *J*-*V* curves of the $CsPbBr_3$ PSCs doped with (a) NaSCN and (b) KSCN under reverse and forward scanning. Hysteresis index (H-index) = ($PCE_{reverse}$ - $PCE_{forward}$)/$PCE_{reverse}$ × 100%.

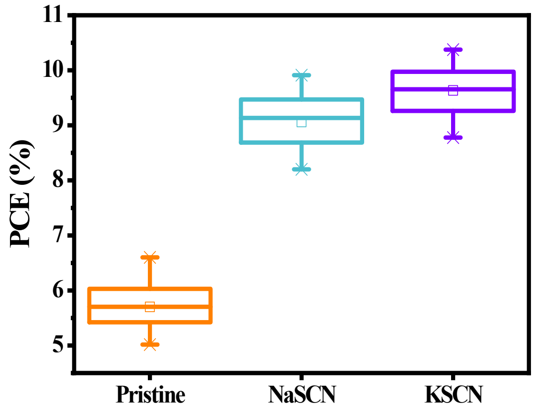

Fig. S9 The statistical distribution of PCE for different HTM-free $CsPbBr_3$ PSCs.

Table S1. TRPL decay carrier lifetimes parameters of excitonic transitions for various $CsPbBr_3$ films deposited on glass.

Devices	τ_1 (ns)	τ_2 (ns)	A_1	A_2	τ_{ave} (ns)
Pristine	0.11	3.97	72.12％	27.88％	0.15
with NaSCN	0.15	5.45	75.82％	24.18％	0.22
with KSCN	0.15	5.47	73.14％	26.86％	0.24

Table S2. Photovoltaic parameters of carbon-based HTM-free $CsPbBr_3$ PSCs with NaSCN dopant at different molar ratio.

Devices	J_{SC} (mA cm^{-2})	V_{OC} (V)	FF (%)	PCE (%)
1% NaSCN	7.45	1.509	75.11	8.44
3% NaSCN	7.61	1.621	80.35	9.91
5% NaSCN	7.32	1.477	76.21	8.23
7% NaSCN	7.14	1.468	74.49	7.88

Table S3. Photovoltaic parameters of carbon-based HTM-free $CsPbBr_3$ PSCs with KSCN dopant at different molar ratio.

Devices	J_{SC} (mA cm^{-2})	V_{OC} (V)	FF (%)	PCE (%)
1% KSCN	7.29	1.488	75.48	8.18
3% KSCN	7.42	1.522	78.61	8.87
5% KSCN	7.74	1.624	82.57	10.38
7% KSCN	7.31	1.521	76.79	8.53

Table S4. Summary of the photovoltaic parameters of the state-of-the-art $CsPbBr_3$ PSCs.

Cell configuration	V_{OC} (V)	J_{SC} (mA cm^{-2})	FF (%)	PCE (%)	Ref.
FTO/c-TiO_2/m-TiO_2/$CsPbBr_3$-Na(K)SCN/Carbon	**1.624**	**7.74**	**82.57**	**10.38**	**This work**
FTO/c-TiO_2/m-TiO_2/ $CsPbBr_3$-$SnBr_2$ /Carbon	1.370	7.66	82.22	8.63	S[1]
FTO/c-TiO_2/m-TiO_2/$CsPbBr_3$/Carbon	1.220	7.40	84.10	7.37	S[2]
FTO/c-TiO_2/m-TiO_2/ $CsPbBr_3$-Co/Carbon	1.380	7.48	84.00	8.37	S[3]
FTO/c-TiO_2/$CsPbBr_3$/spiro-OMeTAD/Au	1.500	5.60	62.00	5.40	S[4]
FTO/c-TiO_2/m-TiO_2/GQDs/$CsPbBr_3$/Carbon	1.458	8.12	82.10	9.72	S[5]
FTO/c-TiO_2/m-TiO_2/$CsPbBr_{2.98}Cl_{0.02}$/ Carbon	1.571	7.47	82.93	9.73	S[6]
ITO/SnO_2/$CsPbBr_3$/PMMA/Carbon	1.580	7.93	76.51	9.60	S[7]
FTO/c-TiO_2/$CsPbBr_3$/Carbon	1.375	7.76	79.31	8.47	S[8]
FTO/Sb-TiO_2/$CsPbBr_3$/Carbon	1.654	6.70	80.40	8.91	S[9]
FTO/c-TiO_2/$CsPbBr_3$/Carbon	1.490	6.89	79.00	8.11	S[10]
FTO/c-TiO_2/$CsPbBr_3$/Carbon	1.510	7.48	84.49	9.55	S[11]
FTO/c-TiO_2/$CsPbBr_3$/Carbon	1.380	8.81	75.00	9.11	S[12]
FTO/c-TiO_2/m-TiO_2/ $CsPb_{9.875}Sn_{0.125}Br_3$/carbon	1.360	8.57	69.00	8.04	S[13]
FTO/c−TiO_2/m-TiO_2/$CsPbBr_3$/Carbon	1.359	8.56	72.00	8.38	S[14]
FTO/c-TiO_2/T-$CsPbBr_3$/Carbon	1.595	7.52	81.41	9.82	S[15]
FTO/ TiO_2/$CsPbBr_3$/Carbon	1.555	7.96	83.00	10.27	S[16]
FTO/c-TiO_2/m-TiO_2/ASF/$CsPbBr_3$/Carbon	1.615	7.47	83.56	10.08	S[17]
FTO/c-TiO_2/m-TiO_2/$CsPbBr_3$/DCC/Carbon	1.611	7.79	80.96	10.16	S[18]

Table S5. The stable output current density and PCE of various carbon-based $CsPbBr_3$ PSCs without HTMs at the voltage of maximum power point in **Fig. 3f**.

Devices	J_{MPP} (mA cm^{-2})	PCE_{MPP} (%)
Pristine	5.80	6.40
with NaSCN	6.87	9.55
with KSCN	7.41	10.23

Table S6. The V_{TFL} and n_{trap} values of various $CsPbBr_3$ films.

Samples	V_{TFL} (V)	n_{trap} (10^{14} cm^{-3})
Pristine	0.383	4.596
with NaSCN	0.197	2.364
with KSCN	0.172	2.064

Table S7. EIS parameters of various carbon-based HTM-free $CsPbBr_3$ PSCs.

Devices	R_s (Ω cm^2)	R_{rec} (Ω cm^2)
Pristine	15.25	47.64
with NaSCN	12.88	67.94
with KSCN	10.29	75.32

Reference

[1] H. Guo, Y. Pei, J. Zhang, C. Cai, K. Zhou, Y. Zhu, Doping with $SnBr_2$ in $CsPbBr_3$ to enhance the efficiency of all-inorganic perovskite solar cells, J. Mater. Chem. C 7 (2019) 11234-11243

[2] D. Huang, P. Xie, Z. Pan, H. Rao, X. Zhong, One-step solution deposition of $CsPbBr_3$ based on precursor engineering for efficient all-inorganic perovskite solar cells, J. Mater. Chem. A 7 (2019) 22420-22428.

[3] C. Wang, Y. Long, X. Liu, S. Fu, J. Wang, J. Zhang, Z. Hu, Y. Zhu, A dual promotion strategy of interface modification and ion doping for efficient and stable carbon-based planar $CsPbBr_3$ perovskite solar cells, J. Mater. Chem. C, 8 (2020) 17211-17221.

[4] Q. A. Akkerman, M. Gandini, F. Di Stasio, P. Rastogi, F. Palazon, G. Bertoni, J. M. Ball, M. Prato, A. Petrozza, L. Manna, Strongly emissive perovskite nanocrystal inks for high-voltage solar cells, Nat. Energy 2 (2016) 16194-16200.

[5] J. Duan, Y. Zhao, B. He, Q. Tang, High-purity inorganic perovskite films for solar cells with 9.72 % efficiency, Angew. Chem., Int. Ed. 57 (2018) 3787-3791.

[6] X. Li, B. He, Z. Gong, J. Zhu, W. Zhang, H. Chen, Y. Duan, Q. Tang, Compositional engineering of chloride ion-doped $CsPbBr_3$ halides for highly efficient and stable all-inorganic perovskite solar cells, Sol. RRL 4 (2020) 2000362.

[7] A. Tong, C. Zhu, H. Yan, C. Zhang, Y. Jin, Y. Wu, F. Cao, J. Wu, W. Sun, Defect control for high-efficiency all-inorganic $CsPbBr_3$ perovskite solar cells via hydrophobic polymer interface passivation, J. Alloy. Compd. 942 (2023) 169084

[8] D. Wang, W. Li, Z. Du, G. Li, W. Sun, J. Wu, Z. Lan, Highly efficient $CsPbBr_3$ planar perovskite solar cells via additive engineering with NH_4SCN, ACS Appl. Mater. Interfaces 12 (2020) 10579-10587.

[9] Y. Xu, J. Duan, X. Yang, J. Du, Y. Wang, Y. Duan, Q. Tang, Lattice-tailored low-temperature processed electron transporting materials boost the open-circuit voltage of planar $CsPbBr_3$ perovskite solar cells up to 1.654 V, J. Mater. Chem. A 8 (2020) 11859-11866.

[10] X. Wan, Z. Yu, W. Tian, F. Huang, S. Jin, X. Yang, Y. Cheng, A. Hagfeldt, L. Sun, Efficient and stable planar all-inorganic perovskite solar cells based on high-quality $CsPbBr_3$ films with controllable morphology, J. Energy Chem. 46 (2019) 8-15.

[11] S. Wang, F. Cao, W. Sun, C. Wang, Z. Yan, N. Wang, Z. Lan, J. Wu, A green Bi-solvent system for processing high-quality $CsPbBr_3$ films in efficient all-inorganic perovskite solar cells, Mater. Today Phy. 22 (2022) 100614.

[12] J. Bi, J. Chang, M. Lei, W. Zhang, F. Meng, G. Wang, T. Facile, Fabrication of high-quality $CsPbBr_3$ perovskite films for high-performance solar cells, ACS Appl. Mater. Interfaces 14 (2022) 48888-48896

[13] G. Wang, J. Bi, J. Chang, M. Lei, H. Zheng, Y. Yan, Bandgap tuning of a $CsPbBr_3$ perovskite with synergistically improved quality via Sn^{2+} doping for

high-performance carbon-based inorganic perovskite solar cells, Inorg. Chem. Front., 9 (2022) 4359-4368

[14] X. Zhao, C. Xu, X. Wang, J. Guo, M. Wu, Construction of multilevel network structured carbon nanofiber counter electrode and back interface engineering in all inorganic HTL-free perovskite solar cells, Colloid. Surface. A., 648 (2022) 129420

[15] Z. Gong, B. He, J. Zhu, X. Yao, S. Wang, H. Chen, Y. Duan, Q. Tang, Tri-Brominated perovskite film management and multiple-ionic defect passivation for highly efficient and stable solar cells, Sol. RRL 5 (2021) 202000819.

[16] Z. Zhang, W. Zhu, T. Han, T. Wang, W. Chai, J. Zhu, H. Xi, D. Chen, G. Lu, P. Dong, J. Zhang, C. Zhang, Y. Hao, Accelerated sequential deposition reaction via crystal orientation engineering for low-temperature, high-efficiency carbon-electrode $CsPbBr_3$ solar cells, Energy Environ. Mater. (0) 2023 e12524.

[17] L. Cui, B. He, Y. Ding, J. Zhu, X. Yao, J. Ti, H. Chen, Y. Duan, Q. Tang, Multifunctional interface modifier ammonium silicofluoride for efficient and stable all-inorganic $CsPbBr_3$ perovskite solar cells, Chem. Eng. J., 431 (2022) 134193.

[18] J. Zhu, Y. Liu, B. He, W. Zhang, L. Cui, S. Wang, H. Chen, Y. Duan, Q. Tang, Efficient interface engineering of N, N'-Dicyclohexylcarbodiimide for stable HTMs-free $CsPbBr_3$ perovskite solar cells with 10.16%-efficiency, Chem. Eng. J. 428 (2022) 131950.